EFFECTS OF CELLULAR GEOMETRY ON CURRENT FLOW DURING A PROPAGATED ACTION POTENTIAL

RONALD W. JOYNER, *Department of Physiology and Biophysics, University of Iowa, Iowa City, Iowa 52242*
MONTE WESTERFIELD AND J. W. MOORE, *Department of Physiology, Duke University Medical Center, Durham, North Carolina 27710 U.S.A.*

ABSTRACT An impulse propagating in a cell with nonuniform geometry sees an increased electrical load at regions of increasing diameter or at branch points with certain morphologies. We present here theoretical and experimental studies on the changes in membrane current and axial current associated with diameter changes. The theoretical studies were done with numerical solutions for cable equations that were generalized to include a varying diameter; the Hodgkin-Huxley equations were used to represent the membrane properties. The experimental studies were done using squid axons with the axial insertion of platinized platinum wires to create a localized region of increased electrical load. As an action potential approaches a region of increased electrical load, the action potential amplitude and rate of rise decrease, but there is a marked increase in the magnitude of the inward sodium current. The time integrals of the inward and outward currents are not constant along the fiber and indicate net inward charge movement at regions subjected to an increased electrical load. Changes in the waveform of the axial current at such a region help to explain the temperature dependence of propagation failure at regions of increasing electrical load.

INTRODUCTION

Changes in the electrical load on a propagating impulse at branch points or in regions of increasing diameter can lead to a decreased safety factor for action potential propagation in nerve cells (Goldstein and Rall, 1974; Ramón et al., 1975; Parnas et al., 1976). This geometrical effect is strongly dependent on temperature (Westerfield et al., 1978) and can, under various experimental conditions, lead to conduction failure in neurons of both vertebrates and invertebrates (Barron and Matthews, 1935; Krnjevic and Miledi, 1959; Raymond and Lettvin, 1969). By using physiological stimulation, indirect evidence has been found for failure of propagation of action potentials at branch points of leech sensory axons (Yau, 1976). Theoretical and experimental work on partially demyelinated axons has shown that propagation failure occurs when the increased electrical load seen by the propagating action potential reaches a critical value, and also that this critical load is a sensitive function of temperature (Davis and Jacobson, 1971; Koles and Rasminsky, 1972; Schauf and Davis, 1974).

To gain more insight into this problem we asked the question: are there significant changes in the membrane current associated with impulse transmission through a region of changing diameter? We describe here how geometrical changes affect the axial and membrane currents

---

Dr. Westerfield's present address is Department of Neurobiology, Harvard Medical School, Boston, Mass. 02115.

of a nonmyelinated axon whose membrane properties are uniform. The results show that abrupt changes in electrical load can significantly alter the time-course and magnitude of these currents. Analysis of the currents has given more insight into the mechanism of propagation failure and has produced some unexpected results concerning net current flows and ionic accumulations in regions of nonuniform morphology. The changes in membrane potential waveform have been previously published (Ramón et al., 1975; Goldstein and Rall, 1974) and are included in this work primarily as a timing reference for the changes in current.

METHODS

We have developed numerical and experimental methods for modeling the propagation of action potentials in a single cell with several distinct geometrical features. The numerical method has been presented in detail elsewhere (Joyner et al., 1978) and is basically an extension of the implicit integration technique of Crank and Nicholson (1947) to solve the set of partial differential equations representing membrane potential as a function of time and distance throughout a single cell that may have a nonuniform radius, branched processes, and inhomogeneous membrane properties. The experimental method is an extension of the techniques of Ramón et al. (1976) to modify the cable properties of squid giant axons with the axial insertion of platinized platinum wires to create a region of increased electrical load.

Simulations

Numerical solutions were obtained for the set of second order partial differential equations representing membrane potential as a function of time and position along the cell. Membrane properties throughout the cell were described by the equations of Hodgkin and Huxley (1952), using a temperature of 16°C. The cable representing the cell was divided into a large number (generally 100) of short segments, each of which was assumed to be isopotential at all times. An impulse was stimulated at the left end and propagated to the right. At each time step, an ionic membrane current was computed for each segment by integrating the kinetic parameters m, n, and h which were calculated from the Hodgkin and Huxley (1952) rate constants and stored for each segment. The potential of a segment at time $t + \Delta t$ was defined by the potential of that segment at time t, the potentials of the adjacent segments at time t and $t + \Delta t$, the ionic current of the segment at time t, and a number of geometrical constants. The set of equations thus defined for all the segments was treated as a matrix equation and the simultaneous solution accomplished by a modification of the Gauss-Seidel elimination technique (Gerald, 1970; Moore et al., 1975; Joyner et al., 1978). The axial current leaving each segment was defined as the difference in potential between that segment and its neighbor to the right, divided by the axoplasmic resistance between the center points of the two segments. Thus the axial current in this paper is expressed in units of milliamperes and is defined as positive in the direction of propagation (left to right).

Experiments

Giant axons were excised from squid *Loligo pealei* obtained at the Marine Biological Laboratory, Woods Hole, Mass. The axons were cleaned and placed in a lucite chamber that contained continuously flowing, filtered sea water. The temperature of this sea water bath, measured with an immersible thermistor, was controlled by a peltier cooling device. In each experiment a 75-μm platinum wire was platinized for a length of 20 mm and inserted longitudinally into the axon. This axial wire with low surface resistance (3.0–4.6 Ω cm^2, referred to the membrane area of an equal length of axon with a 500-μm diam) shunted the axoplasmic resistance in 450 to 575 μm axons and produced an isopotential region whose surface area was equivalent to a sphere where diameter was six times that of the axon. The

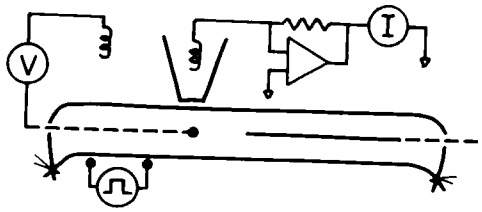

FIGURE 1 Diagram of experimental setup. The platinum axial wire inserted from the right end of the axon has a platinized region (solid part of line) but is otherwise insulated with a thin coat of wax (broken line). A small glass cannula is inserted into the left end of the axon and serves as a movable probe to record the membrane potential at its open end. A movable patch electrode pressed against the outside of the axon measures local membrane current.

transmembrane potential in various regions of the nerve in and near the low resistance axial wire was monitored with an intracellular axial probe electrode, while simultaneous measurements of local membrane currents were obtained with a patch electrode modified from the technique of Frank and Tauc (1964). The diameter of the patch electrode was between 50 and 150 μm. Charge movements were calculated by graphically integrating the inward and outward phases of the recorded membrane current. Action potentials were elicited by stimulating the nerve with current pulses delivered through a pair of extracellular electrodes (Fig. 1).

RESULTS

Simulations

Fig. 2 shows the effects of an abrupt diameter increase on membrane potential (solid lines), membrane current (dashed lines), and axial current (dotted lines). The vertical scale of 0 to 100 corresponds to 100 mV (membrane potential), 0.004 mA (axial current), or 1 mA/cm^2 (membrane current). For this simulation, the axon is assumed to have a diameter of 100 μm from the point of stimulation up to the point at which the diameter abruptly changes to 550 μm. The variables are plotted as functions of time for three locations along the axon. The upper set of traces corresponds to a point in the center of the axon region with a 100-μm diameter and thus serves as a control (an action potential propagating along a fiber of constant diameter). The middle set of traces is for a point just to the left of the diameter increase, and the lower set of traces is for a point just to the right of the diameter increase.

CURRENT AND POTENTIALS For an action potential propagating along a fiber of constant radius (upper traces of Fig. 2), the membrane potential rises rapidly to a value of nearly 100 mV positive to the resting potential. The ionic membrane current (dashed line) shows a brief negative (inward) phase followed by a longer positive (outward) phase. The axial current (dotted line) shows a brief positive phase followed by a longer negative phase (recall that the axial current is defined in such a way as to be positive from left to right, the direction of propagation in these simulations).

The middle traces of Fig. 2 show the changes in these variables as the action potential approaches a region of increased diameter (increased electrical load). The membrane potential rises more slowly and reaches a lower peak amplitude. Nevertheless, the magnitude of the inward ionic current increases dramatically. The axial current also increased in magnitude and the positive part of its waveform becomes similar to that of the membrane

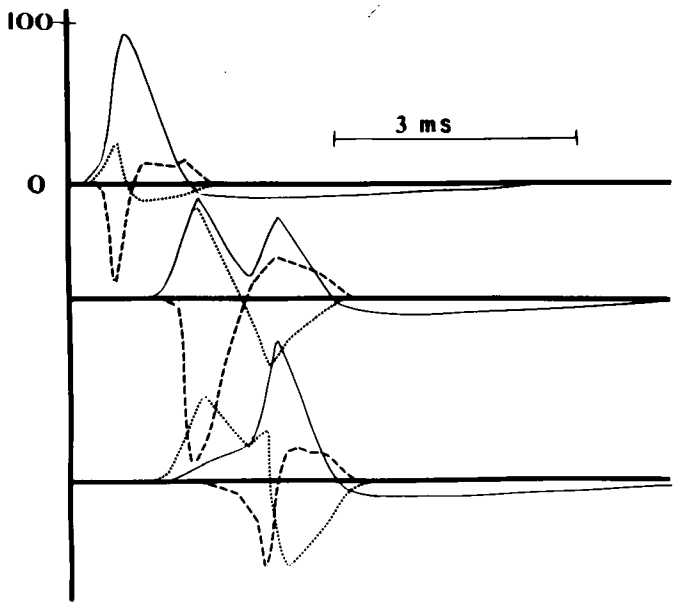

FIGURE 2 Numerical simulations for an axon whose diameter is 100 μm for segments 1–29 and 550 μm for segments 30–60. The axon was stimulated at segment 1 and the membrane potential (solid line), ionic membrane current (dashed line), and the axial current (dotted line) are plotted as functions of time for segments 15, 29, and 31. The vertical scale of 0 to 100 corresponds to 100 mV (membrane potential), 1 mA/cm^2 (membrane current), or 0.004 mA (axial current). Simulation parameters: segment length, 500 μm; time increment, 5 μs; temperature, 16°C; rate constants in Hodgkin-Huxley equations for 6.3°C are increased with $Q_{10} = 3$.

potential. On the falling phase of the action potential, there is a second depolarization that corresponds in time with the delayed action potential in the segment to the right of the diameter increase. The lower set of traces shows the segment just to the right of the diameter increase, where the action potential has a long delay before its regenerative response and has a slightly decreased amplitude. Similarly, the ionic membrane current for this segment is delayed in time and has a slightly decreased magnitude. Both phases of the axial current are increased over normal values.

Because we are using the equations of Hodgkin and Huxley (1952) to represent the axon membrane, we can dissect the changes in the membrane currents into the individual current contributions of sodium and potassium ions. I(Na) and I(K) represent the sodium and potassium membrane currents, respectively (units of mA/cm^2). For a propagated action potential, I(Na) is always negative and I(K) is always positive due to their respective equilibrium potentials. I(total) is the sum of these plus a small leakage current.

Fig. 3 shows I(Na), I(K), and I(total) as functions of time for two segments. The upper part gives the variables as functions of time for an action potential propagating along a uniform axon of 100 μm diam. The lower part shows these variables for a segment just to the left of a diameter increase from 100 to 400 μm. In the uniform axon I(Na) has two distinct peaks in its waveform; but near the transition, the initial peak magnitude of I(Na) is increased and the

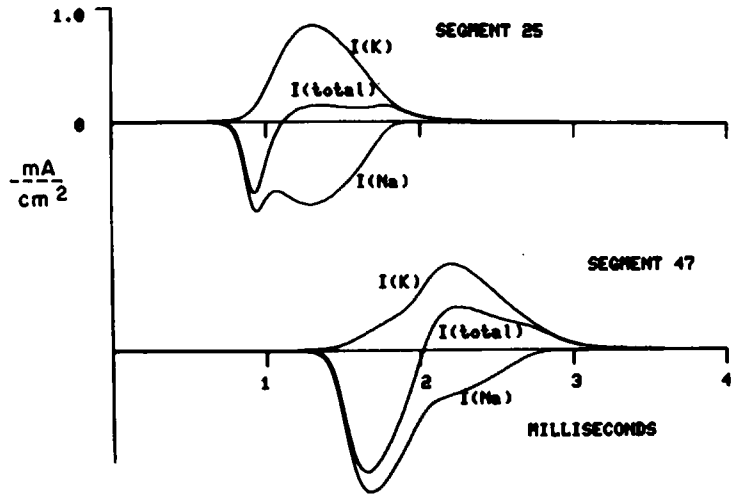

FIGURE 3 Numerical simulations showing I(Na), I(K), and I(total) as functions of time for two segments of an axon with a 100-μm diam for segments 1–49 and a 400-μm diam for segments 50–100. Simulation parameters: segment length, 200 μm; time increment, 2μs; temperature, 16°C; and rate constants in Hodgkin-Huxley equations increased with $Q_{10} = 3$.

second peak is masked or diminished. The time integral of I(Na) is significantly increased in the transition region. Near the transition, I(K) is delayed and decreased, but the change in the time-course is such that its time integral is increased.

IONIC CHARGE MOVEMENTS For an action potential propagating along a fiber of constant diameter, the time integral of ionic membrane current for any segment is zero, with the time integrals of I(Na) and I(K) being nearly equal in magnitude but opposite in sign. The time integrals of I(Na) and I(K) for uniform axon (upper part of Fig. 3) are -5.78 and 6.33 pmol/cm^2, respectively (integrals performed over a 20-ms period that includes one propagating impulse; the negative sign indicates inward flux). Inclusion of the leakage charge of -0.55 pmol/cm^2 brings the total charge movement nearly to zero. However, when the diameter is not constant (or where there is a changing electrical load for other reasons), the individual ionic currents are changed in different ways and the time integral of I(total) is not necessarily zero for each segment of the cell. Fig. 4 shows the time integrals of I(Na), I(K), I(leak), and I(total) as functions of distance along an axon. The simulated axon has a diameter of 100 μm for segments 1–49 and a diameter of 400 μm for segments 50–100. With a spatial increment of 200 μm, the transition occurs at a distance of 10 mm from the point of stimulation. Just to the left of the transition, there is an increase in the net movement of potassium and sodium, but the increases occur with different shapes and magnitudes, and (since the time integral of the leakage current is nearly constant along the fiber) the integral of I(total) along the axon deviates from zero. As the action potential approaches the transitional region, a small net charge loss precedes a large net charge entry followed by a second small net charge loss beyond the transition region. Changes in potassium net flux dominate the total charge movement between 6 and 8.5 mm, while changes in sodium flux dominate in the region from 8.5 to 10 mm.

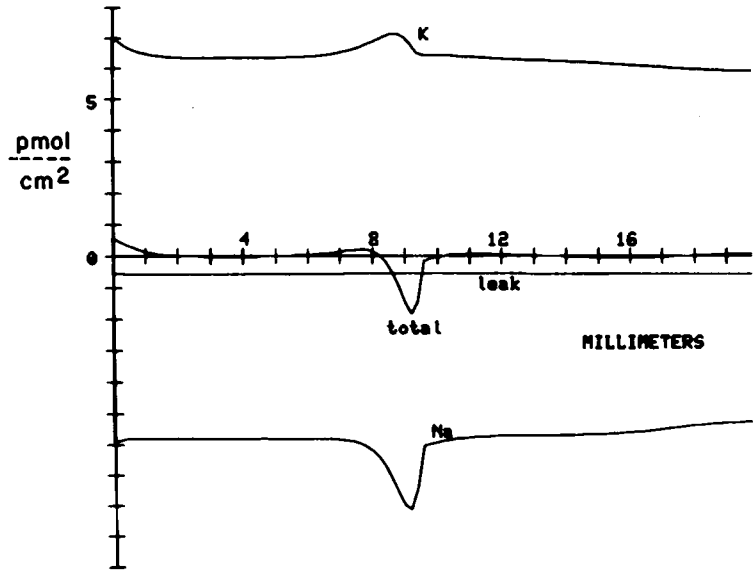

FIGURE 4 Numerical simulation showing the time integrals of I(Na), I(K), and I(leak), and I(total) as functions of distance along the axon described for Fig. 3.

Experiments

The membrane currents associated with the impulses conducted in squid giant axons are dramatically distorted by a change in the internal resistance of the nerve. This effect is illustrated in Fig. 5, which shows the local membrane current recorded at several locations along the surface of an axon in one experiment. As the impulse propagated through the normal axonal region (upper part of the figure), toward that containing the axial wire (lower part of the figure), several changes were observed in the current waveforms. In the region 6 mm or less from the end of the wire, the inward component of the current developed a shoulder on its falling phase. As the impulse moved closer to the end of the wire, the shoulder became larger and occurred sooner after the initial peak of the inward current. At 1 mm from the end of the wire, the shoulder and peak superimposed, producing a large increase in the magnitude of the peak inward current. In the nine experiments in which these observations were made, the peak inward component increased two to four fold in the region near the end of the axial wire, while the magnitude of the outward current phase increased slightly in each case.

The right side of the figure shows the results of a simulation of an axon with a regional decrease in internal resistivity, R_i, using the same temperature, axon diameter, and wire length as in the experiment. These membrane currents (ionic plus capacitive) are plotted at 1-mm intervals. The simulations predict the major changes in the currents observed at different locations from the end of the wire, including the increased amplitude of the inward phase. There are some clear differences between the experimental and simulated waveforms. The length of axon over which the currents were affected by the wire was about one-third longer in the experimental records; also, there was a prominent negative "bump" on the decline of the inward current phase that was not reproduced in the simulations. This "bump"

was synchronous with the activation of the large membrane region around the wire. Further modeling to recreate this effect might require a more detailed representation of the electrical characteristics of the wire and also of the properties of the Schwann cell sheath surrounding the axon.

Very significant changes in the membrane current waveforms are seen at considerable distances from the end of the wire, even when the action potential waveform is minimally changed. This effect is more dramatic at low temperatures where there is a greater safety factor and less distortion of the action potential by changes in electrical load (Westerfield et

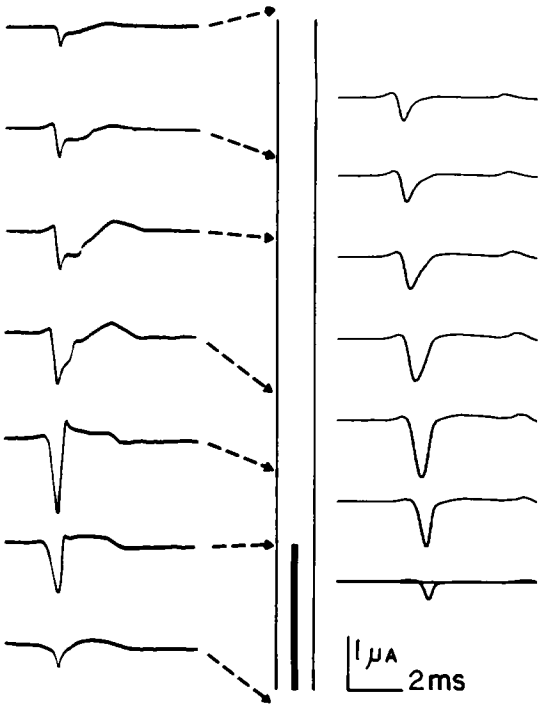

FIGURE 5

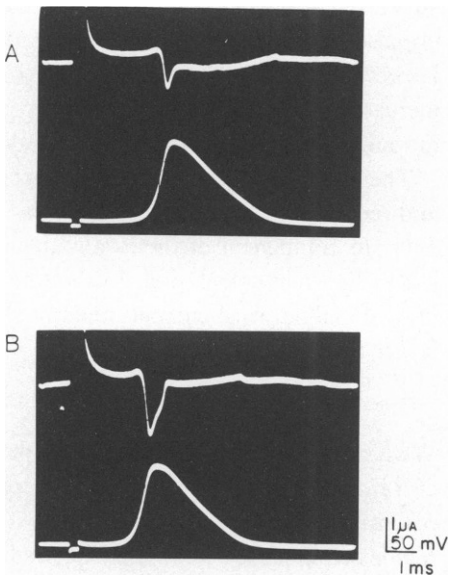

FIGURE 6

FIGURE 5 Experimental and theoretical membrane currents at various locations along an axon with an internal wire as shown. The simulated currents (ionic plus capacitive) were calculated for an axon of 500 μm diam with the wire region of length 2 cm modeled by a regional reduction of R_i from 35.4 to 1 Ω cm. The currents are plotted on the right for segments 1 mm apart. The experimental records were obtained with the patch electrode positioned along the axon as indicated by the arrows. The impulse propagated from top to bottom. The experimental axon diameter was 500 μm; wire resistance, 4.6 Ω cm^2; and temperature, 2°C. The vertical calibration of 1 μA applies only to the experimental records with a corresponding value of 0.74 mA/cm^2 for the simulated currents. Patch electrode lumen was ~100 μm diam.

FIGURE 6 Experimental records of membrane current and potential from two locations along an axon, showing that the membrane current is a more sensitive detector of an axial wire in the circuitry than is the shape of the action potential. (*A*) Normal uniform axon, 25 mm from the top of an axial platinum wire, shows the normal membrane current (upper trace) and the transmembrane potential (lower trace). (*B*) 3 mm from the tip of the wire shows a normal action potential but a dramatically changed membrane current. Axon diameter is 450 μm; wire resistance, 3 Ω cm^2; temperature, 3°C.

al., 1978). This phenomenon is illustrated in Fig. 6, which shows records (at 3°C) of the propagated action potential and membrane currents obtained at the same location by positioning the extracellular current electrode directly over the intracellular potential electrode. Fig. 6 *A* shows the normal membrane current (upper trace) and potential (lower trace) in a uniform axon 25 mm from the end of the axial wire, and Fig. 6 *B* shows a dramatic increase in the inward current phase 3 mm from the end of the wire.

The inward and outward charge movements associated with propagated action potentials increased at the transition from high to low internal resistivity. In general, the inward charge movement increased more than the outward, averaging (in four experiments) three times larger than normal near the transition from high to low internal resistivity. The outward charge movement increased only 1.5-fold, on the average. Although the current records of Figs. 5 and 6 show a significant amount of noise that restricted the accuracy of measurement of charge movement, a strong temperature dependence of charge movement near the end of the axial wire was clearly seen. Fig. 7 *A* shows how, at 26°C, both inward (circles) and outward (triangles) components of charge movement increased four to five times as the impulse approached the end of the axial wire (as diagrammed at the top of the figure). However, when the nerve was cooled to 2°C (Fig. 7 *B*), the inward charge movement (circles) increased only about two-fold near the end of the same wire. The resolution of outward charge movement (triangles) was insufficient to make a definitive statement.

The length of axon used in these experiments limited the distance between the stimulating and recording electrode to 5 cm or less, so that the stimulus artifact often affected the initial outward component of the local current. For this reason the initial outward component was not included in calculations of the total outward charge and resulted in an inequality of the inward and outward current integrals. In Fig. 7, the net inward charge movement was always larger than the outward.

DISCUSSION

We have described here how an abrupt increase in diameter changes the membrane and axial currents in an axon, associated with previously reported changes in the shape of the action potential. The changes in current provide insight into the mechanism of propagation failure at regions of increased electrical load, and also help in our understanding of why the critical ratio for failure is strongly dependent on temperature (Westerfield et al., 1978).

As an impulse propagating in an axon approaches a transition to a larger diameter, it encounters an increasing electrical load. It must charge a larger capacity through a reduced axial resistance. Even at some distance away, an impulse begins to provide extra current without appreciable attenuation of the action potential amplitude. As the impulse comes closer to the abrupt increase in diameter, its ability to provide this depolarizing current may become strained by the heavier load, producing a slower rise of the action potential and an attenuated amplitude. This simply reflects the fact that the internal or source impedance of the active patch is no longer low compared with its load. This reduction of the peak membrane potential and the increase in duration of the rising phase causes a more than normal influx of sodium ions because the driving force ($V - E_{na}$) remains large, providing the required additional charge for depolarizing the adjacent region of increased diameter (Figs. 2 and 3).

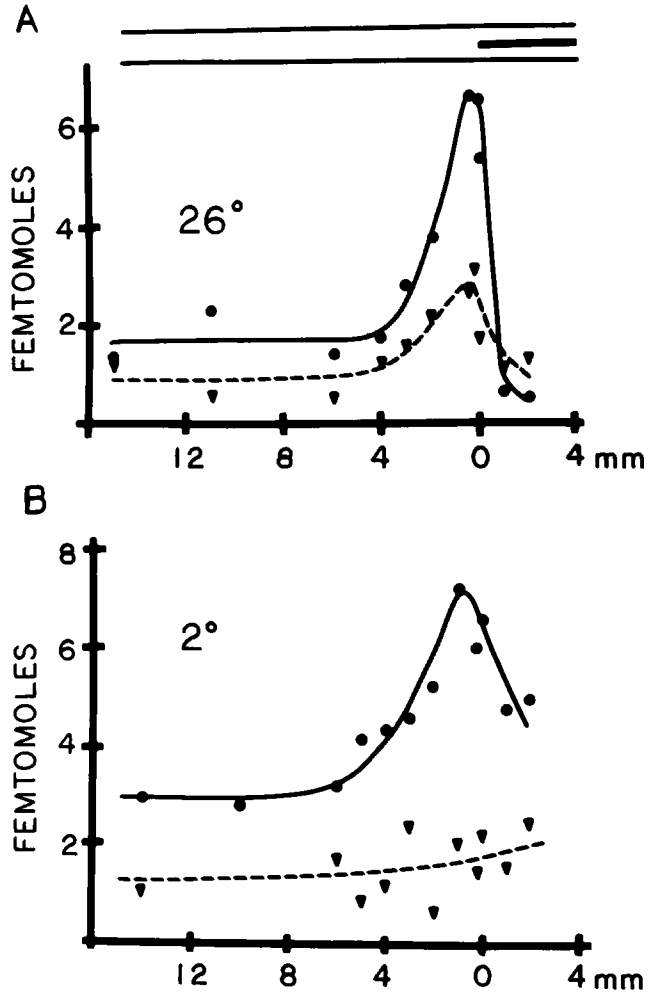

FIGURE 7 Membrane charge transfer during a propagated impulse as a function of temperature and changes in axial resistance. The total charge in femtomoles (10^{-15} mol) associated with propagation of an impulse along the normal axon into the region containing the axial wire is shown as a function of distance from the end of the wire (shown schematically at the top of the figure). The circles and solid curves are the charge movements calculated from measurements of the integrals of the inward current phases of the recorded membrane current, while the triangles and broken curves were calculated from the outward phases. The temperature was 26°C in *A* and 2°C in *B*. The axon diameter was 500 μm and the resistance of the wire 4.5 Ω cm^2.

The large depolarization arising during the falling phase of the action potential (center of Fig. 2) in the segment of the small axon immediately adjacent to the large diameter region reflects the ease with which the latter can affect its neighbor. This is because of a much lower effective internal (source) impedance of the large diameter region resulting from the 5.5-fold increase in membrane area and the thirty-fold reduction in axial resistance per unit length.

These changes in amplitude and duration of the inward and outward currents bring about local changes in the net ionic movements. An appreciable excess of sodium enters the axon just to the left of the change in diameter. However, this is not enough to cause a significant change in the local internal concentration of sodium ions in any but the smallest axons, and diffusion will quickly redistribute the excess. With impulse conduction, there is also an excess movement of potassium ions into the space around the small axon in the region to the left of the diameter change. If diffusion is restricted by a Schwann cell layer or close packing of other cells in this region, the local change in external potassium ion concentration may become significant (Frankenhaeuser and Hodgkin, 1956). The effect will become more pronounced with a closely spaced train of impulses (Frankenhaeuser and Hodgkin, 1956; Adelman and FitzHugh, 1975). Such an increase in extracellular potassium concentration will lead to a local depolarization of the membrane, which further affects and complicates the propagation of the impulse through the transitional region.

Although we find that the net charge movement during a propagated impulse may deviate from zero near a change in diameter, there is conservation of charge for the cell as a whole. When the charge movements shown in Fig. 4 were integrated over the total length of the axon, the sodium, potassium, and leakage movements balanced to within one part in one thousand (within the accuracy of the simulation).

The temperature dependence of propagation failure can be understood in terms of the changes produced in the axial current near a point of increasing electrical load. As an impulse approaches an abrupt increase in diameter (e.g., center of Fig. 2), the initial phase of the axial current waveform approaches that of the action potential. This axial current provides the "stimulus" for the region of increased diameter, and the stimulating charge transferred is simply the time integral of the axial current. Although the spike amplitude is rather temperature insensitive, its duration has a Q_{10} of $\sim 1/2.4$ (Hodgkin and Katz, 1949; Westerfield et al., 1978). Thus, the amount of charge available to stimulate the region of larger diameter increases with action potential duration. As an axon is cooled, the capability of an impulse to supply stimulating current to the region ahead is enhanced so that larger electrical loads (larger diameter increases) can be excited and the probability of failure decreased.

Our studies make clear that the concept of the "safety factor" for propagation is much more complex than merely the ratio of the action potential amplitude to the threshold potential. It should be defined in terms of the ability of the action potential to continue propagation in spite of some obstacle, such as a region of increased electrical load. Perhaps a better way to discuss the safety factor for propagation is in terms of the ratio of depolarizing charge that a segment of axon can supply to a neighboring region divided by the charge necessary for the excitation of that region.

The observations presented here demand caution in the interpretation of local membrane current observations. Such measurements are used frequently to assess the relative density of ionic channels in the membrane of various parts of a cell. The complexities brought on by geometry must be considered in any careful interpretation (for example, the records of Fig. 5 might be interpreted to indicate the presence of a greater density of ionic channels in the region near the end of the axial wire, even though this is not the case).

In summary, the observations presented here clarify the mechanism of failure of conduction of a single impulse approaching an increased electrical load. Both the simulations and the experiments show that the inward membrane current increases markedly in segments adjacent to an increased electrical load, even though the action potential magnitude and its rate of rise decrease. The larger ionic charge transfers and possible accumulation could lower further the safety factor for successive action potentials in a train. One problem in investigation the "filtering" or integrative effects at branch points or other regions of increased electrical load is that the best description of the membrane excitability properties, the Hodgkin-Huxley equations, were formulated for short term (ten ms or less) conductance studies, and there are little data describing slower conductance changes.

We appreciate the assistance of Mr. E. M. Harris in maintaining the instrumentation. We are indebted to Dr. N. Stockbridge for some of the computer simulations. This work was supported by National Institutes of Health grants NS03437 and NS11613 to Dr. Moore and HL22562 and NS15350 to Dr. Joyner. The experimental work was carried out at the Marine Biological Laboratory, Woods Hole, Mass.

Received for publication 17 December 1979 and in revised form 21 April 1980.

REFERENCES

ADELMAN, W. J., and R. FITZHUGH. 1975. Solutions of the Hodgkin-Huxley equations modified for potassium accumulation in a periaxonal space. *Fed. Proc.* **34**:1322.

BARRON, D. H., and B. H. C. MATTHEWS. 1935. Intermittent conduction in the spinal cord. *J. Physiol. (Lond.).* **85**:73–103.

CRANK, J., and P. NICOLSON. 1947. A practical method for numerical evaluation of solutions of partial differential equations of the heat-conduction type. *Proc. Cambridge Phil. Soc.* **43**:50–67.

DAVIS, F. A., and S. JACOBSON. 1971 Altered thermal sensitivity in injured and demyelinated nerve. A possible model of temperature effects in multiple sclerosis. *J. Neurol. Neurosurg. Psychiatry.* **34**:551–561.

FRANK, K., and L. TAUC. 1964. Voltage clamp studies on molluscan neuron membrane properties. *In* The Cellular Functions of Membrane Transport. J. F. Hoffman, editor. Prentiss-Hall, Inc., Englewood, N.J.

FRANKENHAEUSER, B., and A. L. HODGKIN. 1956. The after effects of impulses in the giant nerve fibres of *Loligo. J. Physiol. (Lond.).* **131**:341.

GERALD, C. F. 1970. Applied numerical analysis. Addison-Wesley Publishing Company, Inc., Reading, Mass.

GOLDSTEIN, S., and W. RALL. 1974. Changes of action potential shape and velocity for changing core conductor geometry. *Biophys. J.* **14**:731.

HODGKIN, A. L., and A. F. HUXLEY. 1952. Current carried by sodium and potassium ions through the membrane of the giant axon of *Loligo. J. Physiol. (Lond.).* **116**:449–472.

HODGKIN, A. L., and B. KATZ. 1949. The effect of temperature on the electrical activity of the giant axon of the squid. *J. Physiol. (Lond.).* **108**:33–77.

JOYNER, R. W., M. WESTERFIELD, J. W. MOORE, and N. STOCKBRIDGE. 1978. A numerical method to model excitable cells. *Biophys. J.* **22**:155–170.

KOLES, Z. J., and M. RASMINSKY. 1972. A computer simulation of conduction in demyelinated nerve fibers. *J. Physiol. (Lond.).* **227**:351–364.

KRNJEVIC, K., and R. MILEDI. 1959. Presynaptic failure of neuromuscular propagation in rats. *J. Physiol. (Lond.).* **149**:1–22.

MOORE, J. W., F. RAMÓN, and R. W. JOYNER. 1975. Axon voltage-clamp simulations. I. Methods and tests. *Biophys. J.* **15**:11.

PARNAS, I., S. HOCHSTEIN, and H. PARNAS. 1976. Theoretical analysis of parameters leading to frequency modulation along an inhomogeneous axon. *J. Neurophysiol.* **39**:909–923.

RAMÓN, F., R. W. JOYNER, and J. W. MOORE. 1975. Propagation of action potentials in inhomogeneous axon regions. *Fed. Proc.* **34**:1357.

RAMÓN, F., J. W. MOORE, R. W. JOYNER, and M. WESTERFIELD. 1976. Squid giant axons. A model for the neuron soma? *Biophys. J.* **16**:953.

RAYMOND, S. A., and J. Y. LETTVIN. 1969. Influences on axonal conduction. *Quart. Prog. Rep Res. Lab. Electr. M.I.T.* **92**:431–435.

SCHAUF, C. L., and F. A. DAVIS. 1974. Impulse conduction in multiple sclerosis. *J. Neurol. Neurosurg. Psychiatry.* **37**:152–161.

WESTERFIELD, M., R. W. JOYNER, and J. W. MOORE. 1978. Temperature-sensitive conduction failure at axon branch points. *J. Neurophysiol. (Bethesda).* **41**:108.

YAU, K. 1976. Receptive fields, geometry and conduction block of sensory neurones in the central nervous system of the leech. *J. Physiol. (Lond.).* **263**:513–538.